Use of computational fluid dynamics for the calculation of ship resistance, and its variation with the ship hull form parameters

Adel A. Banawan and Yasser M. Ahmed
Marine Eng. and Naval Architecture Dept., Faculty of Eng., Alexandria University, Alexandria, Egypt

The practical application of the Computational Fluid Dynamics (CFD), for predicting the flow pattern around ship hull has made much progress over the last decade. Today, several of the CFD tools play an important role in the ship hull form design. In this paper CFD has been used for calculating ship resistance, and investigating its variation when changing the ship hull form due to varying the ship hull form parameters, which represents a very important task in the principal and final design stages.

إن التطبيق العملي لاستخدام الديناميكا العددية لتوقع خصائص وشكل المانع حول بدن السفينة قد شهد تقدم كبير في العقد الأخير. تلعب اليوم العديد من برامج الديناميكا العددية دور كبير فى عملية تصميم بدن السفينة. هذا البحث تم فيه استخدام الديناميكا العددية لحساب معاوقة السفينة وتحرى تغيرها عند تغير بدن السفينة نتيجة لتغير معاملات بدن السفينة وهذا يمثل هدف مهم جدا في مرحلة التصميم الأساسية والنهائية للسفينة.

Keywords: CFD, Ship resistance, Ship hull form, Hull form parameters, SSPA series models

1. Introduction

Although model testing will continue to be a very important method in determining the resistance and power requirements in the future, CFD has recently been recognized as a useful tool at principal and final design stages. CFD is economical in time and cost in comparison with the experimental methods, and allow the designer to estimate and predict some characteristics of the flow pattern around the ship hull form which are not possible to be obtained by model tests.

However, in order to use the computational method, CFD, as a useful tool for hull form design, the CFD results must be credible and accurate enough, and can forecast the changes in the flow pattern characteristics accompanied by the hull form variations.

The studies to improve the CFD technology for the prediction of flow characteristics around ship hull form have been actively carried out in the world through the International CFD Workshops which were held four times in last two decades (Larsson, 1980, Larsson et al. 1991, Kodama, 1994, Larsson et al. 2000) [1].

At present, several of CFD codes play an important role in the ship hull form design. In particular non-linear free surface potential flow codes for predicting ship wave pattern are widely used at institutes and shipyards over the past years. These potential flow codes are good and efficient and can give a good anticipation of the quality of the hull form design from the wave making resistance point of view (Raven, 1998).

In addition to that the use of Reynolds Average Navier Stokes Equations (RANSE), solvers for predicting the characteristics of the viscous flow around the ship hull form has increased. These provide important new possibilities such as forecasting wake fields, local flow directions, thrust deduction…etc. Consequently, the improvements of the ship hull form can be achieved.

In this study the ship resistance is calculated using CFD. The study is also focused on investigating the effects of varying ship hull form parameters *L/B, LCB* and C_B hull parameters upon the viscous resistance and wave making resistance of the Cargo Liner Series (SSPA) models and examined the sensitivity between altering these parameters and the ship resistance.

The viscous resistance of the different models utilized in this study have been calculated numerically using the finite volume

code FLUENT [2], while the wave making resistance of the same models has been predicted and calculated using the potential flow code KELVIN [3].

2. Governing ship flow equations

The coordinate system (x,y,z) for calculating the viscous resistance and the wave making resistance is defined to represent the flow patterns around hull form as positive x in the opposite flow direction, positive y in port side and positive z upward where the origin at the aft perpendicular of the hull form, as shown in fig. 1.

2.1. Governing equations for calculating viscous resistance

Continuity equation:

$$\frac{\partial u_i}{\partial x_i} = 0 . \tag{1}$$

Momentum transport equation:

$$u_j \frac{\partial u_i}{\partial x_i} = -\frac{1}{\rho}\frac{\partial p}{\partial x_i} + \frac{\partial}{\partial x_j}\left[\upsilon\left(\frac{\partial u_i}{\partial x_j} + \frac{\partial u_j}{\partial x_i}\right)\right] + \frac{\partial}{\partial x_j}\left(-\overline{u_i' u_j'}\right), \tag{2}$$

$$-\overline{u_i' u_j'} = \upsilon_t\left(\frac{\partial u_i}{\partial x_j} + \frac{\partial u_j}{\partial x_i}\right) - \frac{2}{3}k\delta_{ij} . \tag{3}$$

Turbulent model equations:

The Renormalization-group (RNG) k-ε turbulent model was used in this study, where

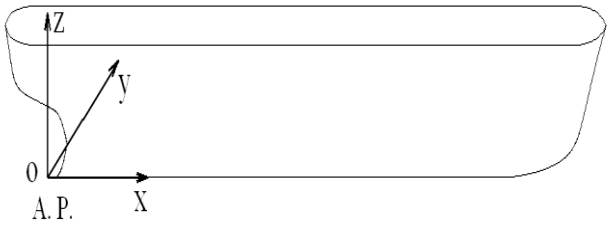

Fig. 1. Coordinate system.

$$\rho u_j \frac{\partial k_i}{\partial x_j} = \frac{\partial}{\partial x_i}\left[\alpha_k \mu_{eff}\frac{\partial k}{\partial x_i}\right] + G_k + G_b - \rho\varepsilon - Y_M , \tag{4}$$

and

$$\rho u_j \frac{\partial \varepsilon_i}{\partial x_j} = \frac{\partial}{\partial x_i}\left[\alpha_\varepsilon \mu_{eff}\frac{\partial \varepsilon}{\partial x_i}\right] + C_{1\varepsilon}\frac{\varepsilon}{k}(G_k + G_{3\varepsilon}G_b) - C_{2\varepsilon}\rho\frac{\varepsilon^2}{k} - R , \tag{5}$$

where G_k, , G_b and Y_M are the generation of turbulent kinetic energy due the mean velocity gradients, the generation of turbulent kinetic energy due to buoyancy and the contribution of the fluctuating dilatation in compressible turbulence to the overall dissipation rate. The model constants $G_{1\varepsilon}$, $G_{2\varepsilon}$, α_k and α_ε, in this study have taken the following values

$G_{1\varepsilon}$ = 1.42; $G_{2\varepsilon}$ = 1.68 and α_k = α_ε = 1.39.

2.2. Governing equations of wave making resistance

Continuity equation:

$$\nabla^2\phi = \frac{\partial^2\phi}{\partial x^2} + \frac{\partial^2\phi}{\partial y^2} + \frac{\partial^2\phi}{\partial z^2} = 0 . \tag{6}$$

Water surface condition:

$$\frac{1}{2}\nabla\phi\nabla(\nabla\phi)^2 + g\phi_z = 0 . \tag{7}$$

Ship hull surface condition:

$$\vec{n}.\nabla\phi = 0 . \tag{8}$$

3. Computational method

3.1. Computational method for viscous resistance

To solve the governing equations, the fluid domain is subdivided into a finite number of cells and these equations are changed into algebraic form via discretisation process. Finite volume method is used for the discretisation. The convective terms are

discretised using Second Order Upwind scheme, and the pressure is interpolated using Linear interpolation scheme. Central difference scheme is utilized for diffusion terms. For the pressure-velocity coupling the SIMPLE (Semi-Implicit Methods for Pressure-Linked Equation) is utilized [4-6].

The algebraic equations obtained from the discretisation process are solved iteratively. Solution convergence was monitored by dimensionless residual sum for all variables across the computational points. The minimum residual sum for convergence was set to 1×10^{-6}.

3.2. Computational method for wave making resistance

The computational domain "triad" is subdivide into two numerical grids; the numerical grid on the ship hull surface and the numerical grid on the water surface belong to the ship hull. The flow is superimposed from point sources located near to the patch centers and the boundary conditions are satisfied in the average over surface "patches".

During the iterations the non-linear free surface boundary condition is applied. After each iteration, the new ship floating condition and the deformation of the free water surface are calculated. The grid generator generates the numerical grid again on the ship hull surface considering the new floating condition and the new deformation of the free water surface. The numerical grid on the water surface is updated with respect to the calculated wave heights and the calculated waterline. A convergence has been achieved, if the changes of the calculated deformation of the free water surface and the calculated wave making resistance are less than a certain criteria for each one.

4. Boundary conditions

4.1. Boundary conditions for viscous resistance

Wall function is utilized for hull surface boundary condition. Symmetry boundary condition is applied for the center plane and the water free surface by assuming double body model. Uniform flow conditions at the inlet and exit planes are applied. The velocities are applied parallel to the opposite direction to the x axis [4].

4.2. Boundary conditions for wave making resistance

The non-linear boundary condition and the radiation condition (in this condition the waves created by the ship do not propagate ahead of it) are applied at the water surface. Additionally, the boundary condition at the wetted ship hull surface is that water can not penetrate the ship hull surface.

5. Investigated hull forms

In this study the selected hull forms have been chosen from the SSPA series models, and they are categorized into three main groups:

- The length-beam ratio, L/B, variation group,
- The position of LCB variation group,
- The block coefficient, C_B, variation group.

The longitudinal dimensions of the parent form, Model No. 720, were multiplied by a constant factor a, while all the transverse and vertical dimensions were multiplied by $1/\sqrt{a}$ in order to obtain Models Nos. 809, 810 and 811 of the L/B variation group table 1. The body plan and the contour of the parent form, Model No. 720, are shown in fig. 2 [7].

In the LCB variation group, the new forms were derived from the parent form, Model No. 720, with a method called swinging of sectional area curve [7a]. The main specifications of the models of this group can be obtained from table 2 and the body plans of the Models Nos. 822-824, are given in fig. 3 [7].

Models Nos. 632, 824 and the modified Model No. 799 have been chosen for the analysis of block coefficient variation group. The basic data of these models can be found in table 3. The lines and resistance data of the modified Model No. 799 have been obtained according to the overall analysis of the SSPA Cargo Linear Series presented by A. Shaher Sabit in references [9] and [10]. The body plans of Models Nos. 632 and the modified 799 are shown in fig. 4.

6. Grid generation

All the models and their computational domains were meshed using tetrahedral cells for calculating viscous resistance. The number of cells is about

Table 1
The main dimensions of L/B variation group

Model No.	809	810	720	811
Model scale	1:20			
a	0.90	0.95	1.00	1.05
L (m)	110.70	116.85	123.00	129.15
L_{pp} (m)	108.00	114.00	120.00	126.00
B (m)	17.92	17.44	17.00	16.59
T (m)	7.446	7.267	7.083	6.912
$\nabla(m^3)$	9750			
L/B	6.18	6.70	7.24	7.79
B/T (m)	2.4			
LCB	-0.75%			
C_B	0.675			
C_M	0.984			

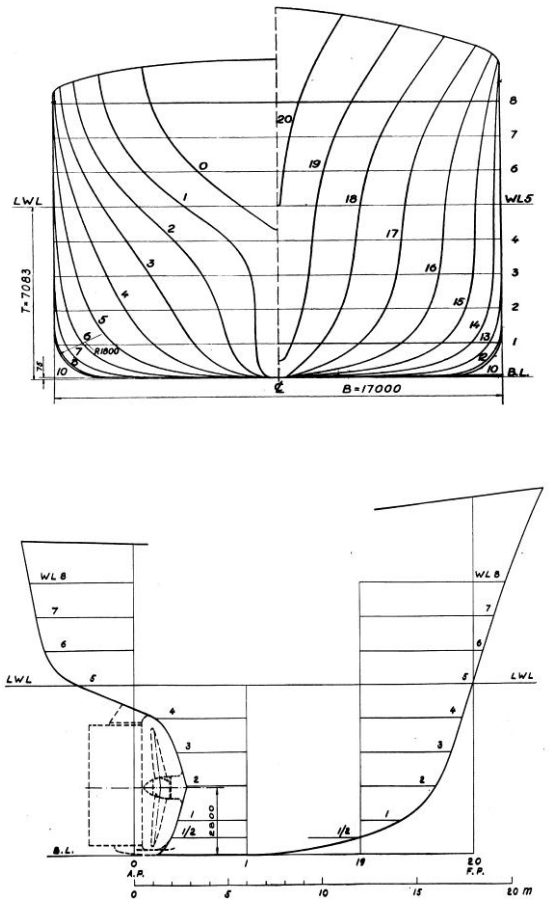

Fig. 2. Body plan of model no. 720 and its bow and stern contours [7].

Table 2
The main dimensions of LCB variation group

Model No.	822	720	323	824
Model scale	1:20			
L (m)	123.00			
L_{pp} (m)	120			
B (m)	17.00			
T (m)	7.083			
$\nabla(m^3)$	950			
L/B	7.24			
B/T (m)	2.40			
LCB	0%	-0.75%	-1.35%	-2.00
C_B	0.675			
C_M	0.984			

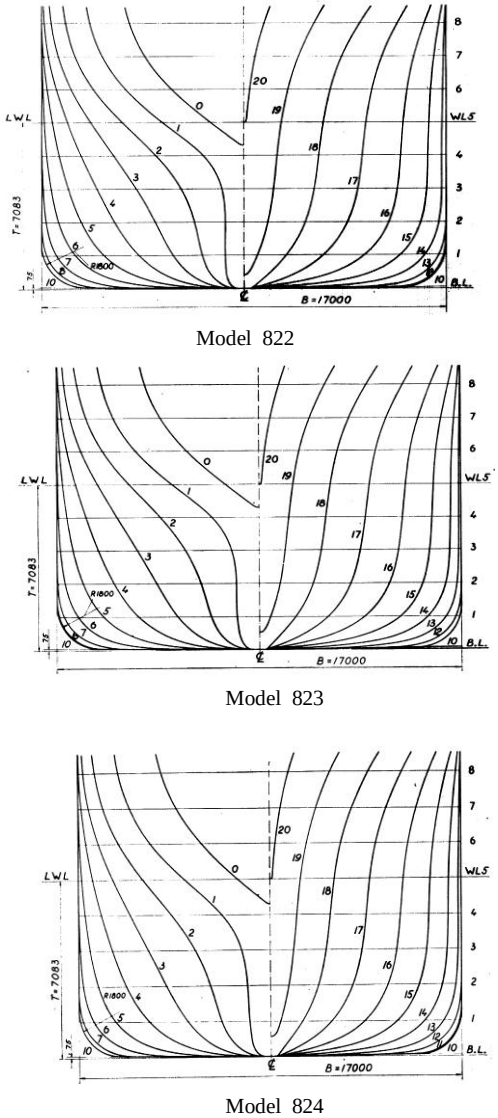

Fig. 3. Body plan of models nos. 822, 823 and 824 [7].

Table 3
The main dimensions of C_B variation group

Model No.	632	824	Modified 799
Model scale	1:20		
L (m)	123.00		
L_{pp} *(m)*	120.00		
B (m)	17.00		
T (m)	7.083		
V(m^3)	7586	9750	10476
L/B	7.24		
B/T (m)	2.4		
LCB	-2.00%		
C_B	0.525	0.675	0.725
C_M	0.95	9.984	0.984

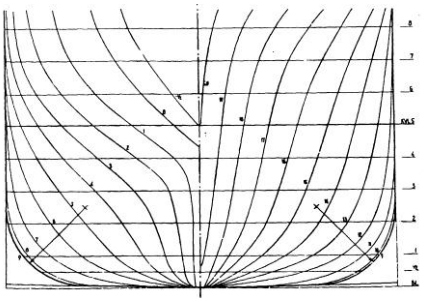

Model 632

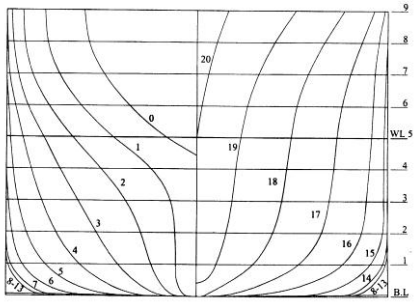

Model M799

Fig. 4. Body plans of model no. 632 (C_B = 0.525) and the modified model no. M799 (C_B = 0.725)

513154 in the computational domains of the length-beam ratio, *L/B*, variation group and the position of *LCB* variation group models. While, the computational mesh was made from nearly 480569 grid cells for the computational domains of Model No. 632 and about 498384 for the modified Model No. 799.

The quadrilateral patches were applied for meshing the ship hull surface and water surface for calculating the ship wave making resistance. The numbers of patches were based on the velocity under consideration.

7. Ship resistance results

The numerical method results of this study are based on the following:

The total resistance is divided into viscous resistance, R_v, and wave making resistance, R_w, hence

- $R_T = R_V + R_w \Rightarrow C_T = C_v + C_w$
- The calculations based on the full scale, to avoid the existence of laminar flow.

While the experimental results of the models of the SSPA Cargo Linear Series depended on:

The total resistance is divided into frictional resistance, R_F, and residuary resistance, R_R, hence

- $R_T = R_F + R_R \Rightarrow C_T = C_F + C_R$
- The model-scale results from the resistance tests were converted to the scale of the full-size by using Froude method of extrapolation.

7.1. The length-beam ratio, L/B, variation group

The experimental results of this group illustrate that as *L/B* ratio increases the total resistance coefficient, C_T, decreases and vice versa. In fact, the rate of diminishing of C_T with respect to *L/B* ratio is rather high, which indicates the significance of this hull form parameter.

The numerical results of the study show excellent agreement with the conception stated above, as shown in fig. 5. Actually, the principal causes of the inverse relationship between varying *L/B* ratio of the hull form and the ship resistance can be summarised as follows:

1. The viscous resistance coefficient, C_v, increases with the decreases of *L/B* ratio (due to mainly the increase in the viscous pressure resistance), as shown in fig. 6. The decrease of *L/B* ratio leads to vary the features of the hull form wetted part, hence the pressure distribution and gradient around the hull form will be altered. As a result, the velocity vectors show diminishing in their values at the stern region due to the increase in the pressure and the

effect of boundary layer there. Finally, the C_v increases as L/B decreases.

2. The wave making resistance coefficient, C_w, decreases with the increase of L/B ratio, as shown from fig. 7. The reduction of C_w occurs because of the variations associated with the increase of L/B ratio on the shape of load water line and the under water part of the hull form. Consequently, the wave heights of

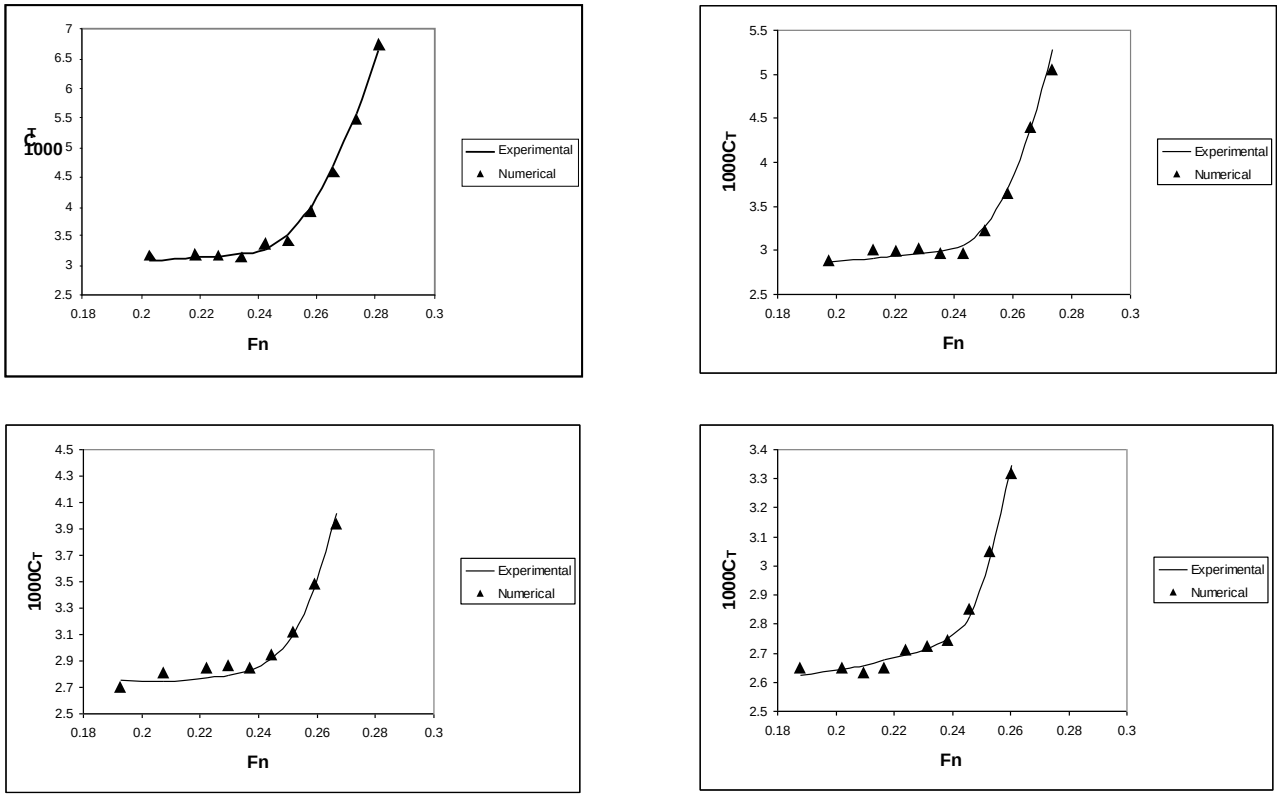

Fig. 5. Experimental and numerical C_T versus F_n of Models Nos. 809 (L/B = 6.18), 810 (L/B = 6.70), 720 (L/B = 7.24) and 811 (L/B = 7.79).

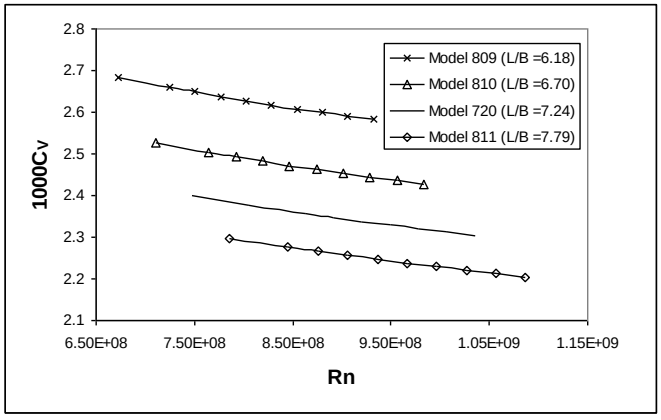

Fig. 6. Numerical results of C_v for L/B variation group models.

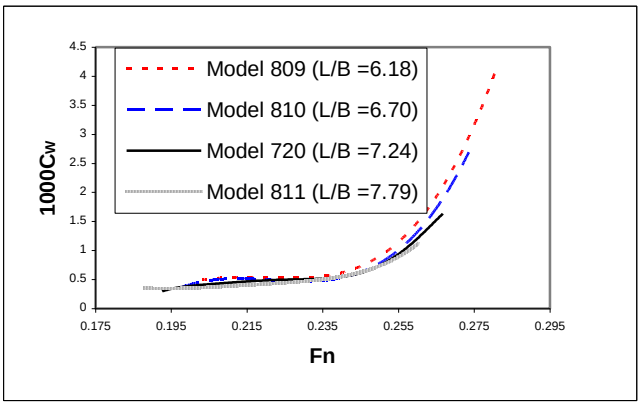

Fig. 7. Numerical results of C_w for L/B variation group models represented by polynomial curves.

the wave pattern formed by the hull form will be reduced.

7.2. The position of LCB variation group

Generally, the resistance tests for the different models showed that there is an optimum position of *LCB* with each F_n or speed. Additionally, resistance tests results of Models Nos. 822, 720, 823 and 824 belong to this group show that a more aft position of the *LCB* is favourable in the higher range of Froude number, F_n, while a more forward position of the *LCB* is better in the low range of F_n.

In fact, the results obtained in this investigation of the models of this group are in harmony with the experimental outcomes of them, as can be clearly seen from fig. 8. The resistance tests of the models of this group have been carried out with rudders, whereas the numerical calculations of these models have been done without rudders.

The analysis of this research work regarding the models of this group shows the following:

1. An increase in the value of C_v at the same R_n with the further aft movement of the position of *LCB*, as shown in fig. 9. Actually, the more astern movement of *LCB* makes the after part of the hull form comparatively fuller than the forward part of the same hull form. As a result, the pressure will be dropped in the forward region and raised in the after region. These changes in the pressure distribution cause an augmentation in the value of viscous pressure resistance component, which is considered to be the major reason of increasing the viscous resistance of the hull form.
2. The prime effect of varying the position of *LCB* is on C_w. At high F_n, high speeds, the value of C_w, declines with the astern movement of *LCB* and vice versa, as can be noted from fig. 10. This occurs due to the fall in the pressure at the forward area as a consequence of moving *LCB* aft and the decrease in the value of half angle of entrance. These causes meliorate the wave pattern produced by the hull form and decrease the wave heights at the bow of this wave pattern. However, at lower Froude numbers the situation is reversed where the wave making resistance will rise with the further aft movement of the position of *LCB*. This befalls because at the lower speeds, the viscous resistance becomes prevailing, and this will directly influence on the wave patterns produced at these lower speeds.

7.3. The block coefficient, C_B, variation group

Indeed, it has been found that the rate of increase of ship resistance with respect to the block coefficient, C_B, is quite high indicating the high effect of this parameter.

The study results of this group models are in consistence with their experimental outcomes, as illustrated in fig. 11 (the numerical calculations of this group models have been carried out without rudders).

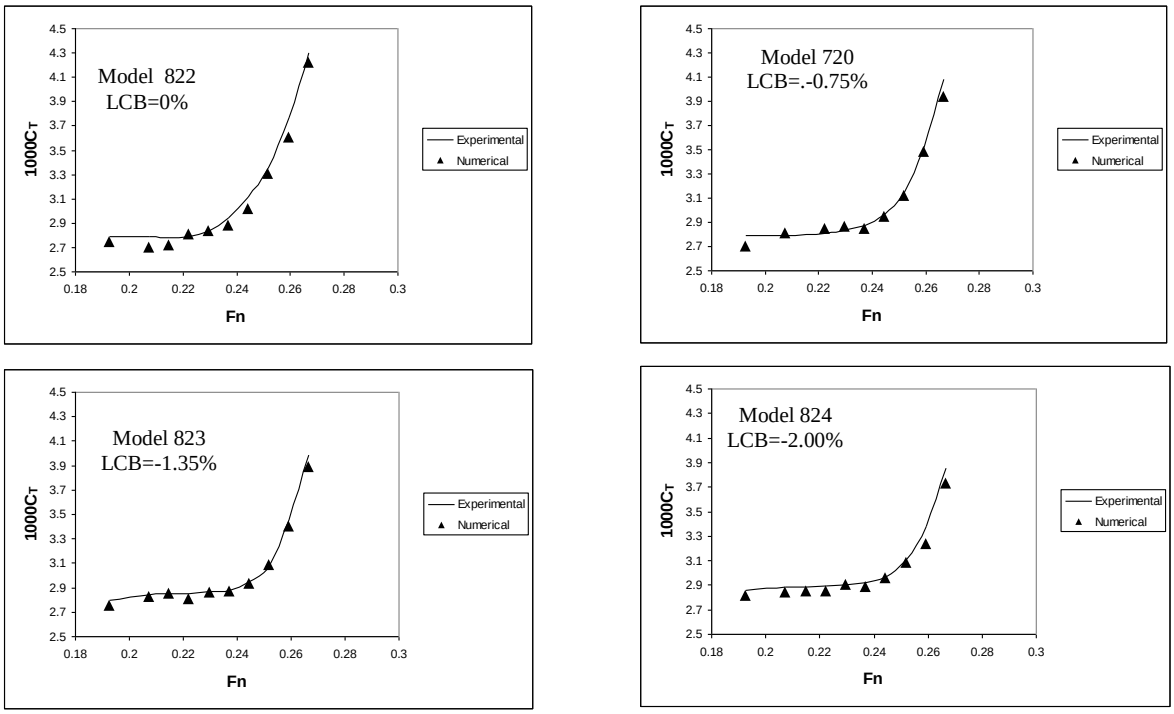

Fig. 8. Experimental and numerical C_T versus F_n of Models Nos. 822, 720, 823 and 824.

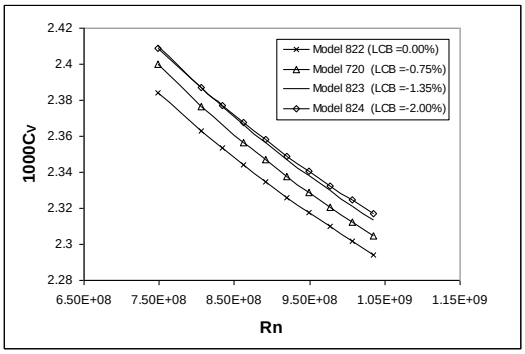

Fig. 9. Numerical result s of C_v for *LCB* variation group models.

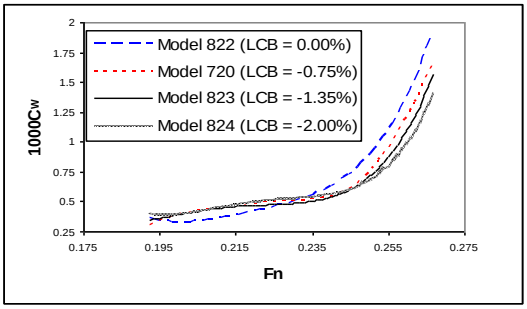

Fig. 10. Numerical results of *Cw* for *LCB* variation group models represented by polynomial curves.

It has been found the main reasons of the high rate increase of ship resistance with block coefficient are due to:

1. The appreciable increment in the value of C_v with the increase of C_B, as shown in fig. 12. This may refer to the increase of C_B leads to an increase in the wetted surface area of the hull form also the hull form lines in this case become more steeper at the fore and aft part, which stimulates a serious alterations in the flow properties around the hull form. These changes in the flow pattern produce an increase in the pressure in the region of bow and fore part of the hull form, as well the pressure gradient at this region affected very much with this raise of C_B. Finally, this will cause an increase in value of frictional resistance and viscous pressure resistance, hence the increase in viscous resistance.
2. The value of C_w highly increases with the increase of C_B, as illustrated in fig. 13. The principal reasons of mounting the wave making resistance with the increment of C_B, has been found due to: The potential changes in the pressure values and distribution around the hull form, the increase in the values of half angle of entrance and the

modifications of the hull form aft part were due to the increase of C_B which influence the wave pattern that is generated by the hull form, leads to increase of C_w.

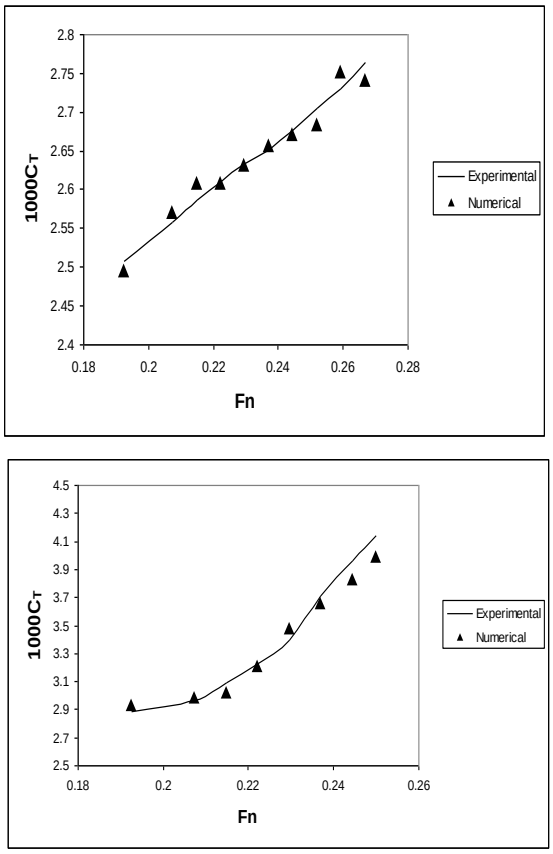

Fig. 11. Experimental and numerical C_T versus F_n of Models Nos. 632 and modified 799.

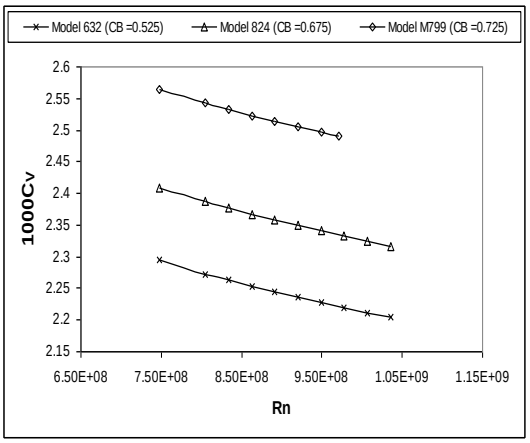

Fig. 12. Numerical results of C_v for C_B variation group models.

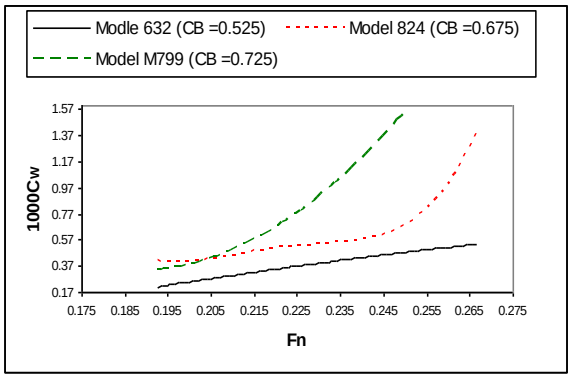

Fig. 13. Numerical results of C_w for C_B variation group models represented by polynomial curves.

8. Conclusions

A number of remarks and observations are concluded from the above work.

1. There is a strong correlation between varying the hull form parameters and the hydrodynamic characteristics of the flow pattern around the ship hull form.
2. The main reasons for the differences between the numerical and experimental results are because of the existence of errors in tank testing, extrapolation process, friction line and the numerical errors in computational method, CFD, which arise during the solution process.
3. The study shows that the increase of L/B ratio leads to a reduction in the value of C_T due to the direct decrease in the values of C_v and C_w. This decline occurs as a result of improving the hydrodynamic properties of the flow pattern around the ship hull form as L/B ratio increases.
4. The change of LCB position has a substantial effect on the value of C_w mostly at high F_n or $V\sqrt{L}$, where the more astern position of LCB is superior in high range of F_n, and the more forward position of LCB is better in the low range of F_n.
5. The variation of hull forms block coefficients, C_B, has a significant effects on the resistance and propulsion qualities of the hull forms.
6. Increasing L/B ratio, moving LCB forward or reducing the value of C_B for the different hull forms reduce the effects of viscous wake upon the velocity field at propeller plane.

Consequently, the Q.P.C becomes better and higher.

7. It is essential during the initial design stage for the designer to make a suitable compromise between the different hull form parameters in order to acquire a good design that fulfills the different design requirements.

References

[1] Gothenburg 2000: http://www. iihr.u. iowa.edu/gothenburg200/

[2] FLUENT Inc. Web Page: http://www.fluent.com/.

[3] SAV-Potsdam Web Page: http://www.sva-potsdam.de/.

[4] H.K. Versteeg, W. Malalasekera, An Introduction to Computational Fluid Dynamics – The Finite Volume Method, Longman Group Ltd. (1995).

[5] B.E. Launder, D.B. Spalding, Lectures in Mathematical Models of Turbulence, Academic Press Inc. (London) Ltd. (1972).

[6] Joel Ferziger, Milovan Peric, Computational Methods for Fluid Dynamics, Springer – Verlag Berlin Heidelberg (1999).

[7] E. Freimanis, Hans Lindgren, "Systematic Tests with Ship Models with C_B = 0.675- Part III- Influence of Main Dimensions and Center of Buoyancy", the SSPA Standard Series Publication, (42) (1958).

[8] R. Munro Smith, Elements of Ship Design, Marine Media Management Ltd. (1995).

[9] A. Shaher Sabit, "An Overall Analysis of The SSPA Cargo Liner Series – Part I – Hull Surface Generation and Geometry of Forms", International Shipbuilding Progress, Vol. 20 (232) (1973).

[10] A. Shaher Sabit, The SSPA Cargo Liner Series Regression Analysis of the Resistance and Propulsive Coefficients, Part II, Det Norske Veritas, Repot pp. 76 – 071 (1976).

Received October 21, 2005
Accepted December 31, 2005